Fatigue Life Estimation for Different Geometrical Configuration of Load-Carrying Cruciform Joint using ABAQUS and Fe-Safe

Estimación del Tiempo de Fatiga para Diferentes Configuraciones Geométricas de Juntas Cruciformes Portadoras de Carga utilizando ABAQUS y Fe-Safe

Estimativa do Tempo de Fadiga para Diferentes Configurações Geométricas de Juntas Cruciformes Portantes usando ABAQUS e Fe-Safe

Zulqarnain Mukhtar Mahmood[1], Muhammad Asif[2][(*)], Syed Asad Ali Zaidi[3]

Summary. - This research paper focuses on the fatigue analysis of load-carrying cruciform joints made up of thick plates, which are crucial components in ship structures. The study investigates the fatigue life of fillet welded cruciform joints using both 2D and 3D geometries. Various loading conditions and boundary conditions are considered, and an elastic-plastic finite element analysis is conducted using ABAQUS 2021. The number of cycles to failure is estimated using Fe-Safe and the strain-based Brown Miller Morrow model. The results, presented through contour plots, Log Life repeats, and Load Range vs. Number of Cycles graphs, reveal the fatigue behavior and failure locations. Additionally, the methodology is validated against experimental data from literature, demonstrating its applicability. The findings provide insights into the fatigue characteristics of load-carrying cruciform joints in thick plates, contributing to enhanced design and reliability in the shipbuilding industry.

Keywords: Load-carrying Cruciform joint, Fatigue analysis, Elastic-Plastic FEA, ABAQUS, Fe-Safe, 2D and 3D Cruciform geometries.

(*) Corresponding Author

[1] Bachelor of Engineering, Department of Naval Architecture, Pakistan Navy Engineering College, National University of Sciences and Technology (Pakistan), zulqarnainmukhtar622@gmail.com, ORCID iD: https://orcid.org/0009-0003-4412-0477

[2] Assistant Professor, Department of Naval Architecture, Pakistan Navy Engineering College, National University of Sciences and Technology (Pakistan), muhammadasif@pnec.nust.edu.pk, ORCID iD: https://orcid.org/0000-0003-4318-8253

[3] Assistant Professor, Department of Mechnaical Engineering, Faculty of Engineering, Islamic University of Madinah (Saudi Arabia), Sali@iu.edu.sa, ORCID iD: https://orcid.org/0000-0001-5457-5684

Z. M. Mahmood, M. Asif, S. A. Ali Zaidi

Resumen. - *Este trabajo de investigación se centra en el análisis de fatiga de uniones cruciformes portadoras de carga formadas por placas gruesas, que son componentes cruciales en las estructuras de los barcos. El estudio investiga la vida a fatiga de uniones cruciformes soldadas en ángulo utilizando geometrías 2D y 3D. Se consideran varias condiciones de carga y condiciones de contorno, y se realiza un análisis de elementos finitos elástico-plástico utilizando ABAQUS 2021. El número de ciclos hasta la falla se estima utilizando Fe-Safe y el modelo Brown Miller Morrow basado en deformaciones. Los resultados, presentados a través de gráficos de contorno, repeticiones de registro de vida y gráficos de rango de carga versus número de ciclos, revelan el comportamiento de fatiga y las ubicaciones de falla. Además, la metodología está validada con datos experimentales de la literatura, lo que demuestra su aplicabilidad. Los hallazgos proporcionan información sobre las características de fatiga de las uniones cruciformes que soportan carga en placas gruesas, lo que contribuye a mejorar el diseño y la confiabilidad en la industria de la construcción naval.*

Palabras clave: *Unión cruciforme portadora de carga, Análisis de fatiga, FEA Elástico-Plástico, ABAQUS, Fe-Safe, Geometrías cruciformes 2D y 3D.*

Resumo. **-** *Este trabalho de pesquisa concentra-se na análise de fadiga de juntas cruciformes de suporte de carga compostas por placas espessas, que são componentes cruciais em estruturas de navios. O estudo investiga a vida à fadiga de juntas cruciformes soldadas em ângulo usando geometrias 2D e 3D. Várias condições de carregamento e condições de contorno são consideradas, e uma análise de elementos finitos elástico-plásticos é conduzida usando ABAQUS 2021. O número de ciclos até a falha é estimado usando Fe-Safe e o modelo Brown Miller Morrow baseado em deformação. Os resultados, apresentados através de gráficos de contorno, repetições de log de vida útil e gráficos de faixa de carga versus número de ciclos, revelam o comportamento da fadiga e os locais de falha. Adicionalmente, a metodologia é validada frente a dados experimentais da literatura, demonstrando sua aplicabilidade. As descobertas fornecem informações sobre as características de fadiga das juntas cruciformes de suporte de carga em chapas grossas, contribuindo para melhorar o design e a confiabilidade na indústria de construção naval.*

Palavras-chave: *Junta cruciforme portante, análise de fadiga, geometrias elástico-plásticas FEA, ABAQUS, Fe-Safe, 2D e 3D cruciformes.*

1. Introduction. - The construction of ships involves various types of connections, including stiffener joints and plate joints, which are predominantly formed through welding processes. Cruciform joints are used to link longitudinal and transverse structural parts of ships, such as the keel, its frames, and bulkheads. These joints are essential for transmitting and distributing loads across the ship's hull, ensuring the vessel's structural integrity and strength. The load-carrying ability of cruciform joint is critical for the ship to endure the numerous forces encountered during operation, such as waves, the currents, and impacts loads. The proper design and construction of cruciform joints is critical to preventing stress concentrations of fatigue, and structural failure.

The intersection of longitudinal and transverse elements of structure in a cruciform joint generates a complicated stress field, with high stress concentrations located in the weld's toe and root. Geometric discontinuities, weld flaws, and residual stresses induced during the fabrication procedure can all contribute to higher stress concentrations. Welding plays a crucial role in the shipbuilding industry, but it also poses the risk of failures occurring in these joints during the ship's commissioned life. Among the significant joints in ship structures are the cruciform welded joints or connections. These joints experience high loads and are critical to the structural integrity of the ship. Therefore, it is essential to conduct a comprehensive fatigue analysis to ensure their reliability and longevity.

Traditional fatigue evaluation techniques, such as nominal stress and hot-spot stress methods, frequently rely on simpler stress estimations that may not adequately represent the intricate stress distributions found in cruciform joints. Furthermore, empirical relationships based on limited data from experiments, like S-N curves or as notch factor methods, may not sufficiently account for the distinctive geometric and material properties of a particular cruciform joints design, potentially leading to discrepancies in fatigue life estimates.

Benefits of FEA include detailed stress analysis include a more in-depth and accurate assessment of the stress distribution inside a cruciform joint, taking into account the intricate geometry, the properties of the material, loading conditions, and weld-specific characteristics like the weld profile, residual stresses, as well as the presence of defects. Engineers can also undertake parametric studies to optimize the joint's design and material properties, and the findings can be tested versus experimental evidence, allowing for the improvement and validation of the models used for analysis to assure better fatigue life forecasts.

The present research paper focuses on the fatigue analysis of fillet welded load-carrying cruciform joints made up of thick plates. The study involves both 2D and 3D geometries, considering various boundary conditions. The analysis is performed using elastic-plastic finite element analysis (FEA) conducted in ABAQUS 2021. The number of cycles to failure is estimated using Fe-Safe and the strain-based Brown Miller Morrow model. To accurately model the behavior of the joints, the material properties of SAE1045 steel are considered.

The findings of this research have significant implications for the shipbuilding industry. Understanding the fatigue behavior of load-carrying cruciform joints in thick plates enables engineers and designers to make informed decisions regarding their design, fabrication, and maintenance. By identifying critical areas prone to fatigue damage and optimizing the joint configurations, the structural integrity and longevity of ships can be enhanced.

Moreover, the research contributes to the broader field of fatigue analysis and structural engineering. The methodology employed in this study can be extended to other types of joints and structures, providing a framework for evaluating fatigue life and enhancing the reliability of various engineering applications. The specific objectives include:

a) Investigating the fatigue behavior of cruciform joints under various loading conditions.

b) Assessing the influence of 2D and 3D geometry and different boundary conditions to investigate the fatigue characteristics, failure locations, and stress distributions within the joints.

c) Estimating the number of cycles to failure using elastic-plastic FEA and the strain-based Brown Miller Morrow model.

d) Validating the proposed methodology by comparing the simulated results with experimental data from the literature.

The contribution of this research is three-fold. Firstly, to analyze the fatigue life of the cruciform joint through the 3D geometry under varying load magnitudes ranging from 480 to 680 MPa. Secondly, to investigate the fatigue performance of the joint through the 2D geometry under different boundary conditions, including axial loading, vertical loading, bending, and combined axial-bending loading. Lastly, to validate the methodology employed in this study by comparing the simulation results with experimental data from the literature.

The significance of this research lies in its contribution to the understanding of fatigue behavior in load-carrying

cruciform joints of thick plates. The findings will aid in the development of more reliable and durable joint designs for ship structures, thereby improving the overall structural integrity and safety of vessels. Furthermore, the research methodology and insights gained can be extended to other applications that involve welded connections subjected to cyclic loading conditions.

The organization of this paper is as follows: Section 2 provides a literature review on fatigue analysis of welded joints and previous studies related to load-carrying cruciform joints. Section 3 describes the methodology employed, including the finite element modeling techniques, material properties, and numerical simulations. Section 4 presents the results and discussions, including contour plots, Log Life repeats, and Load Range vs. Number of Cycles graphs. Section 5 focuses on the validation study by comparing the simulated results with experimental data from the literature. Finally, Section 6 concludes the paper and discusses the implications of the research findings, along with suggestions for future work.

Fatigue refers to the processes that occur when a material is subjected to cyclic stress, resulting in accumulated degradation and, finally, final fracture. Waves produced in oceans are seen as cyclic excitations applied on a ship while it is at sea. These loads have the potential to cause fatigue damage in structures of ships. The forces generated by the ship's movement (such as rolling and pitching), wind movement, and green water motion are eventually transferred to the ship hull through the lashing bridge structure [1]. Modern ship's structure face serious fatigue damage concerns due to increased ship's tonnage capacity and substantial usage of strong steel [2]. As histories and subsequent service experiences have revealed, fatigue and fracture are key failure causes of ships [3]. The most typical problems in marine vessel's structures during operational activities include fatigue fractures, panel's buckling, indents, and rusting. Fatigue damages, in particular, play a vital role in ship structures [4]. See **¡Error! No se encuentra el origen de la referencia.** for phases of fatigue life.
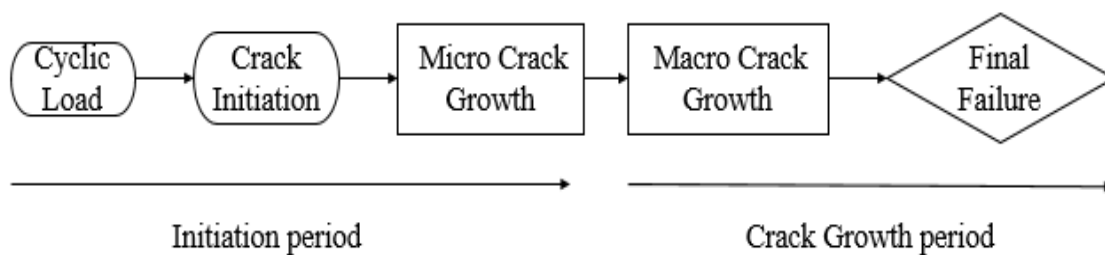

Figure I. Fatigue Life Phases

The plate is a flat structural component having a thin thickness in comparison to its surface size and dimensions. When working with plates, it is common to be perplexed by the subject of how to describe thin or thick plate, or which plate is regarded thicker. According to [5] ratio of thickness to width or thickness to a length less than 10% is regarded as a thin plate, while a ratio higher than 10% is called a thick plate. Thicknesses of thin plates range from $0.1 > t > 0.01$ and thick plates have a thickness (t) higher than 0.01 [6].

Welding is a widely used manufacturing process in shipbuilding, and they are roughly divided into two types: (1) Welding which relies only on heat source, such as fusion welding. (2) Welding which combines heat and pressure sources, such as forge welding [7]. As welding is a fundamental connecting procedure in shipyards, this procedure resulted in welding deformities, which caused numerous issues during the manufacturing of ships [8]. Welding errors can occur because of a welder's inexperience, the use of wrong substances or faulty welding processes, and environmental circumstances [9]. As a large quantity of corrected work is needed, welding imperfections lower the fabrication quality of the ship's hull blocks and lead to poor productive performance [10].

The welded load-carrying cruciform joints (LCJs) are one of the most common connection types in shipbuilding or maritime engineering projects, and fatigue failure to these is a serious hazard to welded constructions [11]. When cruciform joints are exposed to continually changing stresses, they become fatigued [12]. Many types of research have been performed related to fatigue assessment load-carrying cruciform joint (LCJ) and non-load carrying cruciform joint (NLCJ) in literature. This joint is one of the important welded joints for ship structure during ship's construction [13].

Work done by [14] examined the quality of weld and fatigue of NLCJs made by VAG laser and MAG Hybrid welding to produce four lots for testing and find stress concentration factors by applying finite element models with the help of defined parameters of the local geometry of weld. Fatigue of LCJs contain incomplete weld penetration and under-

matching strength of weld deposit and base metal were studied by [15] performing experiments of high and low cycle fatigue on specimens. Research was performed by [16] to analyze fatigue strength affected by the size of cruciform welded joints exposed axial as well as bending stresses. The research in [17] investigates the fatigue modeling or simulation of high-performing steel joints formed by welding by utilizing notched stress and strain-based methods, linear elastic fracture mechanics (LEFM), and SED (strain energy density).

For location of fatigue failure, a study by [18] consider notch stress intensity concept based on William's explanation in LEFM as well as ponder the weld size, transverse plate thickness, incomplete penetration, and plate thickness.

Three geometrically multifarious structural details of the ship were studied and analyzed [19] to estimate their fatigue life using local approaches. All details have communal characteristics like Cruciform joints (two plates crossing each other). A comparative study for fatigue behavior of high cycle fatigue, applied on steel LCJs made by welding was performed by [20] at weld toe and root using PSM (peak stress method) and notch SIF (stress intensity factor). Experimental and theoretical work has been done by [21] to study the effect of cooling and welded bead profile made by shielded metal arc welding process for fatigue life of cruciform joint formed by 8 mm thick plates made up steel ASTM A36 HR.

Some researchers [22] used relationship of RSG (relative stress gradient) and SCF to Notch factor ratio to study the effect caused by the thickness of plates, the radius of weld toe, and bead profile for fatigue of cruciform welded joints. A parametric study for the calculation of notch SCF using spline shape weld model during finite element analyses had performed by [23] for cruciform welded joints experiencing unalike loading scenarios. The research of [24] propose new formulas for SCFs for cruciform joints containing fillet welds subjected to bending loads after employing extended numerical solutions of finite element methods. To study the penetration of weld (full and incomplete) for both fillet welded LCJs and NLCJs had done by [25] with the help of 3D FEM. Strain energy density (SED) approach was used by [26] to investigate parameters like scale effect, bead penetration, length of weld leg, and dimensions of plates for cruciform joints.

Fatigue of fillet welded LCJs made up of austenitic stainless steel investigated by [27] using SN curve, fatigue crack growth, and shape along with prediction method of fatigue life. An evaluation was proposed in [28] to find full fatigue (crack initiation + crack propagation) of cruciform joint prepared by 7005 aluminum alloy considering residual stresses produced after welding. The research work of [29] proposed new equations for SIF at the crack of weld toe for welded LCJ with help of 3D finite element analysis to identify the failure site. To inspect LCF and HCF, a novel energy analytical solution for weld toe and root of welded LCJs made up of 10CrNi3MoV steel was studied in [30] considering the effects of weldment's plasticity and mechanical heterogeneity based on Neuber's Fictitious Notch Rounding concept. The paper [31] re-analyzed the fillet welded LCJs for which failing occur at weld roots and compare results of nominal and notch stress methods for fatigue strength. Some key findings of related research are listed in **Table I**.

Study	Fatigue Analysis Approach	Key Findings
Wei Song et al. [20]	PSM and Notch SIF	A comparative study for fatigue behavior of HCF, applied on steel welded LCJs at weld toe and root.
Oscar and Nelson [21]	Experimental and Theoratical	Find fatigue life due to effect of cooling and welded bead profile made by shielded metal arc welding process.
Toru and Naoki [22]	RSG, SCF and Notch Factor	Study the effects caused by the thickness of plates, the radius of weld toe, and bead profile for fatigue of LCJ
Yixun Wang et al. [23]	Finite Element Analysis	A parametric study for the calculation of notch SCF for fatigue of cruciform joints.
Wang Sub Shin et al. [25]	3D Finite Element Model	Fatigue on the penetration of full and incomplete welded LCJs and NLCJs

Pietro Foti et al. [26]	Strain energy density	Investigate parameters like scale effect, bead penetration, weld leg length, and dimensions of plates for cruciform joints.
Yang Peng et al. [27]	Fatigue life Prediction Method	Fatigue of fillet welded LCJs investigated by using SN curve, fatigue crack growth, and shape.
Jianxiao Ma et al. [28]	Residual Stress Approach	Find full fatigue (crack initiation + crack propagation) of cruciform joint
Haisheng Zhao et al. [29]	3D Finite Element Analysis	Identify the fatigue failure site for welded LCJ.
Wei Song et al. [30]	Neuber's Fictitious Notch Rounding Concept	Inspect LCF and HCF for weld toe and root of welded LCJs made up of 10CrNi3MoV.

Table I. Key Findings of Related Research

The proposed research aims to build upon the existing body of knowledge by conducting a fatigue analysis of load-carrying cruciform joints in thick plates. By employing both 2D and 3D geometries, the study seeks to provide a comprehensive understanding of the fatigue behavior, failure locations, and fatigue life of these joints under various loading conditions. The research findings will contribute to the design and optimization of load-carrying cruciform joints in ship structures, enhancing their fatigue resistance and structural integrity.

2. Methodology. - This section contains the details about what methodology has been used for the present study and it has been applied. It will discuss the joint and software used for the research. It has the following details:

2.1 ABAQUS. - Abaqus, originally known as ABAQUS, was built in 1978 as a simulation software package for studying complex problems utilizing FEA simulations as well as models and designs made with the help of a computer called computer-aided engineering or CAE. This software suite is composed of five core program applications.
Complete ABAQUS Environment (cae) is an application that is employed to make models of physical bodies and investigation of machine-driven parts and systems. It is mostly used for pre-processing designs and models for simulation as well as viewing the results of finite element analysis.
Standard or Implicit, is a common purpose analyzer for finite element analysis using an implicit type of integration strategy. It is a traditionally used tool.
Explicit, used for the distinctive purpose of analyzing finite element problems that investigates highly non - linear problems with several complicated connections under transient loading using an explicit integration approach.
Computational Fluid Dynamics (CFD) is an application used for problems related to fluid dynamics that deliver innovative CFD competencies considering significant pretreatment and post-processing provision.
Electromagnetic, a software tool that is used for computer-based electromagnetic problems that address sophisticated electromagnetic theoretical problems.
ABAQUS is a popular and robust software suite for finite element analysis (FEA) that provides extensive modeling capabilities. Cruciform joints, which frequently display intricate stress distributions and distortion patterns, are a good fit for this analysis method because of its ability to handle non-linear materials, complicated geometries, and a wide range of loading situations. Predicting the fatigue behavior of a joint requires the software to be able to capture the impacts of weld profiles, residual stresses, and various other manufacturing-related parameters on the stress distribution inside the joint. **Figure II** depicts the general solution procedure in ABAQUS.
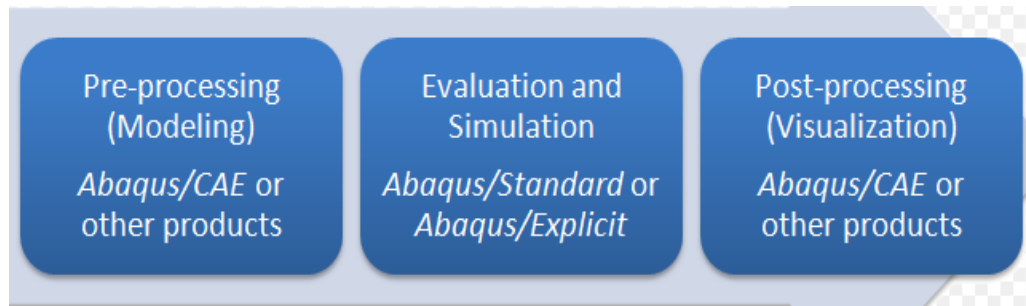
Figure II. ABAQUS General Solution Sequence

2.2 Fe-Safe. - Fe-safe is the industry's first market accessible fatigue analysis program that focuses on current multi-axial strain-based failure methodologies. It is known for its correctness, efficiency, and simplicity of use when analyzing metals, rubber, thermo-mechanical, creep-fatigue, and the welded joints. Fe-Safe is a robust, all-inclusive, and user-friendly package of failure analysis software for models of finite elements. It is used in conjunction with commercialized FEA software packages to determine:

- Occurrence of fatigue cracks
- Estimating the commencing of fatigue cracks
- To find Working stress safety factors
- The chance of survival and persistence at various working lives
- Cracks propagation probability

Fe-Safe will spontaneously select the most suited analytical approach for engineers who may not be fatigue specialists and will approximate material characteristics if test results are not provided. **Figure III** depicts a general fatigue analysis scheme in Fe-Safe.
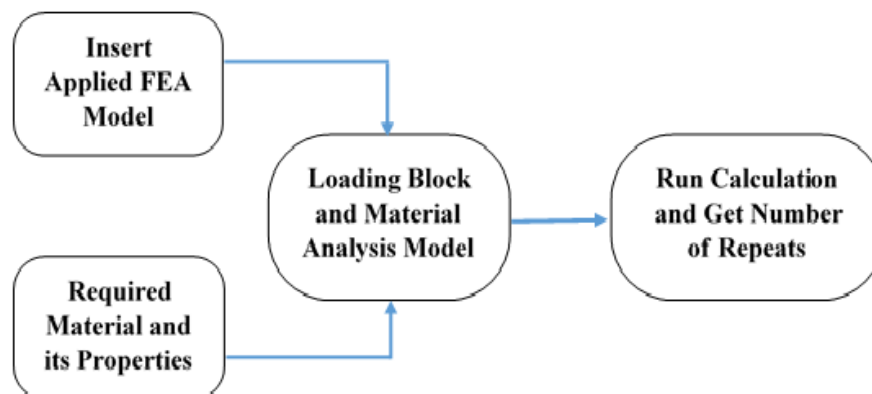

Figure III Fe-Safe Fatigue Analysis General Scheme

2.3 Geometry Used (3D and 2D). - For the investigation, two types of cruciform joint geometry were explored. [25] Gives the dimensions for 3D geometry. **Figure IV** shows an example of this. This geometry includes a 6 mm convex-shaped fillet weld. SolidWorks was used to create a whole (plates + welds) 3D solid model. **Figure V** depicts a SolidWorks model.
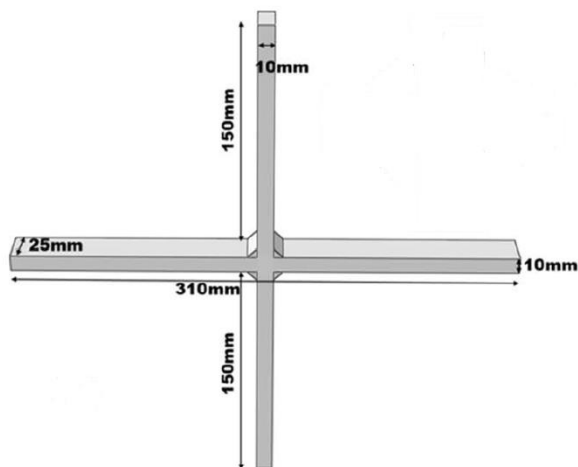
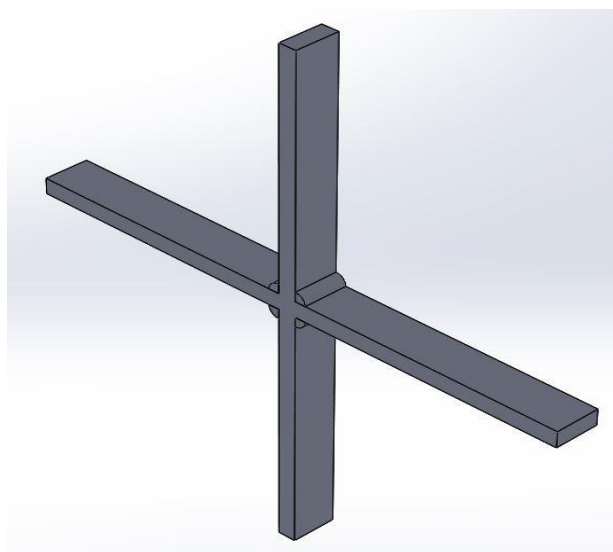*Figure IV. Cruciform Joint 3D Dimensions [25]*

Figure *V.* 3D Model made by SolidWorks.

Dimensions for the 2D geometry of the joint are derived from [32]. **Figure VI** shows an example of this. This shape includes an 8 mm flat fillet weld.
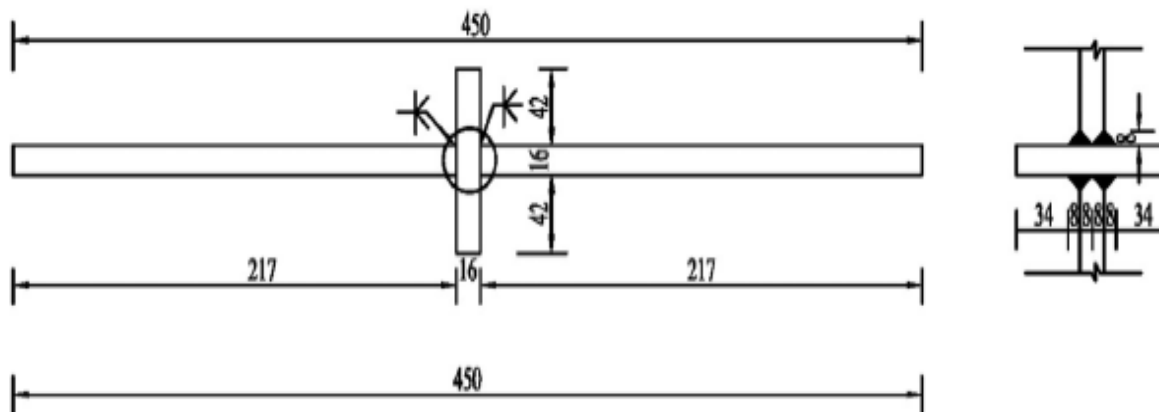

Figure VI. Cruciform Joint 2D Dimensions

This 2D geometry was created in ABAQUS using the part creation feature. 1/4th of geometry was made for axial and vertical loading cases. The rest of the cases are studied on half of the geometry. **Figures 7** and **Figure 8** show ABAQUS 2D models.

Figure VII. 1/4th of the geometry made by ABAQUS.

Figure VIII. Half of the Geometry made by ABAQUS.

2.4 Material for Cruciform Joint. - SAE 1045 is the material used in this study. It is mild carbon steel that is widely utilized in a variety of industries. Axles, bolts, connecting rods, pins, studs, shafts, spindles, and other similar uses are common. It is obvious that these parts are frequently subjected to repeated loading. As a result, increasing the fatigue resistance of SAE 1045 appears to be necessary. SAE 1045's chemical composition is obtained from [33] and is presented in **Table II**.

Constituents	Carbon	Silicon	Manganese	Phosphorus	Sulfur	Iron
Weight %	0.423	0.20	0.56	0.008	0.02	rest

Table II. SAE 1045 Chemical Composition

The monotonic characteristics are achieved [34] by utilizing a 25 KN servo-hydraulic machinery to perform a uniaxial cycle test with a stress ratio of R = -1. During the test, a 2-mm strain gauge was affixed to the specimen to gather strain events. See Figure 3.8 for servo-hydraulic machinery and **Table III** for SAE 1045 monotonic properties.

Properties	Values
Ultimate Tensile Stress (σ_u) (UTS)	798 MPa
Yield Stress (σ_y)	414 MPa
Young's Modulus (E)	198 MPa

Table *III*. SAE 1045 Monotonic Properties

Following that, a cycle test [34] was performed at various percentages of UTS (ultimate tensile strength) acquired from the preceding tensile test. The percentages used are 60, 65, 70, 80, and 85 percent. As a result, five various stress values were used to capture failure time and strain range readings. See Table 3.3 for more information.

Applied Stress (MPa)	Strain Ranges ($\mu\varepsilon$)
480 (60 % of UTS)	2294

520 (65 % of UTS)	3200
570 (70 % of UTS)	4059
640 (80 % of UTS)	4565
680 (85 % of UTS)	5800

Table IV. Applied Stresses for Cyclic Test and Strain Ranges

2.5 Elastic-Plastic FEA. - ABAQUS is used for elastic-plastic finite element analysis. First, a 3D model made by SolidWorks is loaded into ABAQUS, and the 2D geometry of a cruciform joint is created in ABAQUS using the Sketch and Feature tools. Static General STEP is built for plastic analysis after specifying the elastic and plastic material characteristics of SAE 1045. As previously stated, two configurations are being investigated. As a result, for 3D geometry, one type of boundary condition along with axial loadings of 480, 520, 570, 640, and 680 MPa are investigated. One side is fixed, upper and lower face of cruciform joint is allowed to move and the side opposite to fixed side is subjected to axial loading. For more information, see **Figure X**. In the current study, 2D geometry is subjected axial loading for same loading values as of 3D geometry and boundary conditions. For Meshing, an 8-node biquadratic plain strain element CPE8R with reduced integration is utilized. After the work is completed, the findings are taken in the form of stress and deformation contours. The whole flow diagram of elastic-plastic FEA may be found in **Figure IX**.
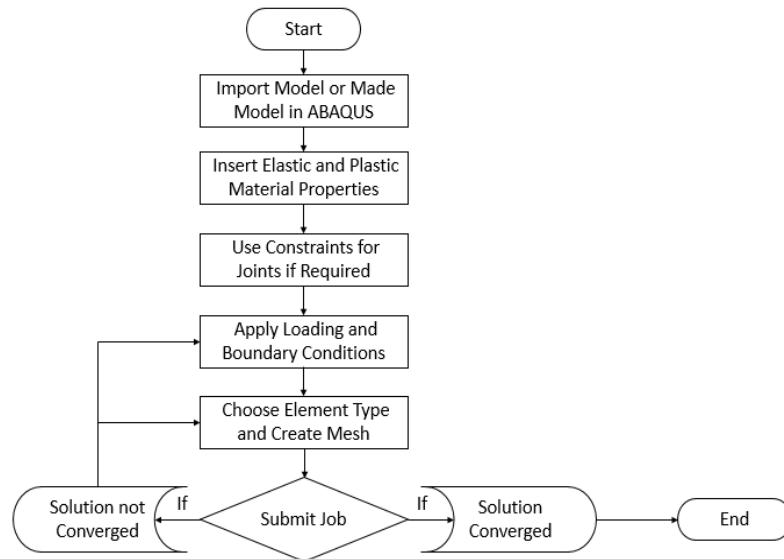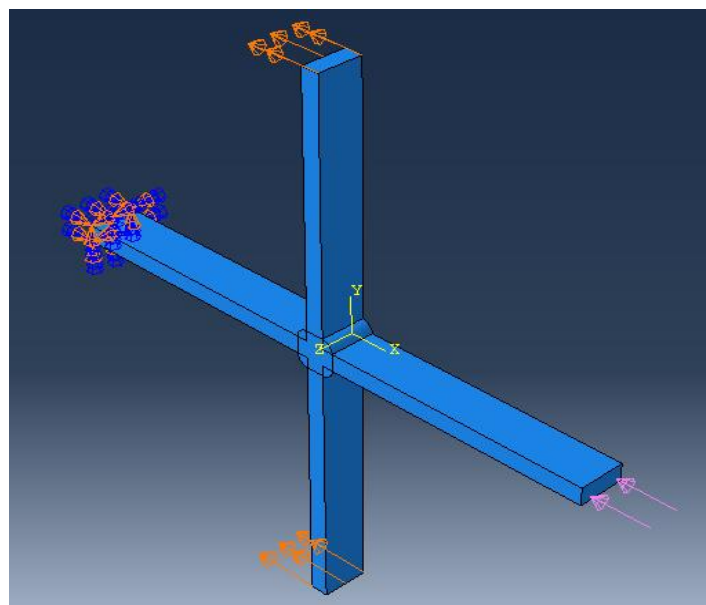

Figure IX. Elastic-Plastic FEA Flowchart

Figure X. Loading Scenario and Boundary Condition for 3D Geometry

2.6 Strain Based Brown Miller Morrow. - According to the Brown-Miller model, much fatigue impairment happens on that plane or surface which is under the influence of the maximum amplitude value of shear strain, and the impairment or failure is an accumulation of both; the shear strain and the strain perpendicular to that plane [35]. See **Figure XI**.
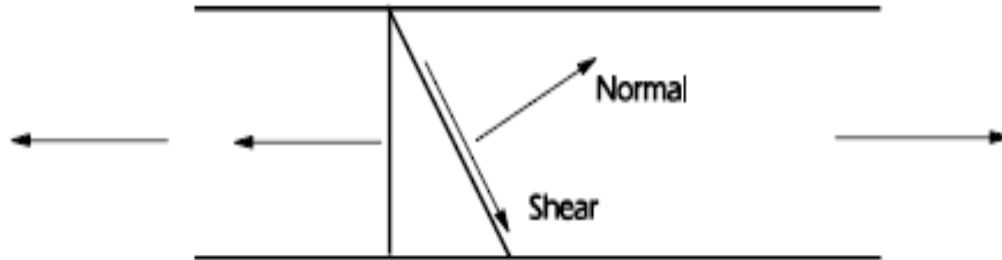

Figure *XI.* Normal and Shear Strain Description [35]

The Brown-Miller model offers the most accurate life predictions for ductile metals but is less accurate for brittle metals. It is a critical plane-based multi-axial fatigue processing algorithm that employs surfaces or planes at a right angle to the surface as well as planes at 45° to the surface. This model focuses on the plane within the material where the likelihood of crack initiation is the highest. It has following key limitations:

- It does not consider non-proportional loadings for fatigue life.
- It lacks to consider mean stress effects on fatigue life.
- It does not explicitly consider progressively accumulation of damage during fatigue.

For materials, it is assumed that the materials are ductile that exhibits plastic deformation before failure. Material is homogenous and isotropic which means that their properties are uniform and does not change direction of loading.

An elastic FEA's stress results are required for this algorithm. To estimate elastic-plastic analysis-based stress strains outcomes from the source of elastic FEA stresses, multi-axial type elastic-plastic based corrections are employed [36].

If

$$\gamma_{max} = Maximum\ Shear\ Strain$$
$$\varepsilon_n = Strain\ Normal\ to\ Maximum\ Shear\ Strain$$

Then from the strain circle of Mohr

$$\frac{\gamma_{max}}{2} = \frac{\varepsilon_1 - \varepsilon_3}{2}$$

And

$$\varepsilon_n = \frac{\varepsilon_1 + \varepsilon_3}{2}$$

In case of uniaxial plain stress

$$\varepsilon_1 = -\upsilon\varepsilon_3$$

And

$$\varepsilon_3 = -\upsilon\varepsilon_1$$

Then

$$\gamma_{max} = \varepsilon_1 - \varepsilon_3 = (1 + \upsilon)\varepsilon_1$$

And

$$\varepsilon_n = \frac{\varepsilon_1 + \varepsilon_3}{2} = \frac{(1 - \upsilon)\varepsilon_1}{2}$$

But, the conservative strain life prediction equation is

$$\frac{\Delta\varepsilon}{2} = \frac{\sigma_f'}{E}(2N_f)^b + \varepsilon_f'(2N_f)^c$$

It can be re-written by considering the amplitudes of shear and normal strains on the left-hand side as

$$\frac{\Delta\gamma_{max}}{2} + \frac{\Delta\varepsilon_n}{2} = C_1 \frac{\sigma_f'}{E}(2N_f)^b + C_2\varepsilon_f'(2N_f)^c$$

Elastic   **Plastic**

For elastic stress cases, the Poisson ratio is

$$v_e = 0.3$$

Then

$$\gamma_{max} = (1 + v_E)\varepsilon_1 = 1.3\ \varepsilon_1$$

Also

$$\varepsilon_n = \frac{(1 - v_E)\varepsilon_1}{2} = 0.35\ \varepsilon_1$$

Then the constant C_1 will be

$$C_1 = 1.3 + 0.35 = 1.65$$

And similarly, for a plastic case, the Poisson ratio is

$$v_p = 0.5$$

Then

$$\gamma_{max} = (1 + v_p)\varepsilon_1 = 1.5\ \varepsilon_1$$

And

$$\varepsilon_n = \frac{(1 - v_p)\varepsilon_1}{2} = 0.25\ \varepsilon_1$$

So, the constant C_2 will be

$$C_2 = 1.5 + 0.25 = 1.75$$

Hence, the complete Brown Miller equation for strain life will become

$$\frac{\Delta\gamma_{max}}{2} + \frac{\Delta\varepsilon_n}{2} = 1.65\frac{\sigma_f'}{E}(2N_f)^b + 1.75\varepsilon_f'(2N_f)^c$$

The researchers Kandil, Brown, and Miller created this version of the Brown-Miller parameter.
The strain-life equation is changed for mean stress correction proposed by Morrow:

$$\frac{\Delta\gamma}{2} + \frac{\Delta\varepsilon_n}{2} = 1.65\frac{\sigma_f'}{E}(2N_f)^b + 1.75\varepsilon_f'(2N_f)^c$$

This approach may also be used to analyze the fatigue of elastic-plastic FEA data [36].

2.7 Fatigue Analysis Using Fe-Safe. - Fe-safe is the industry's first commercially accessible fatigue analysis program that focuses on current multiaxial strain-based fatigue methodologies.
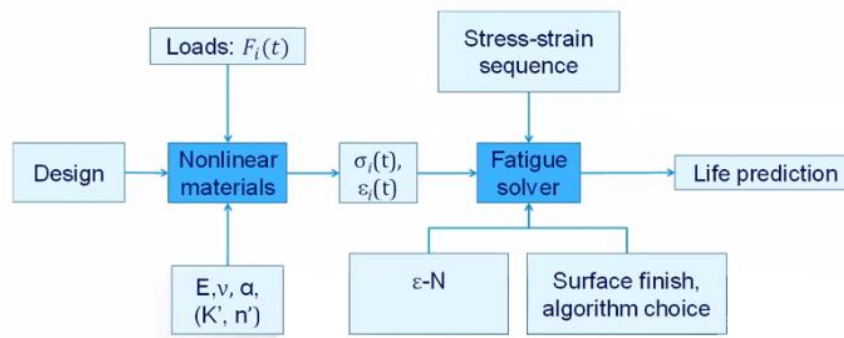
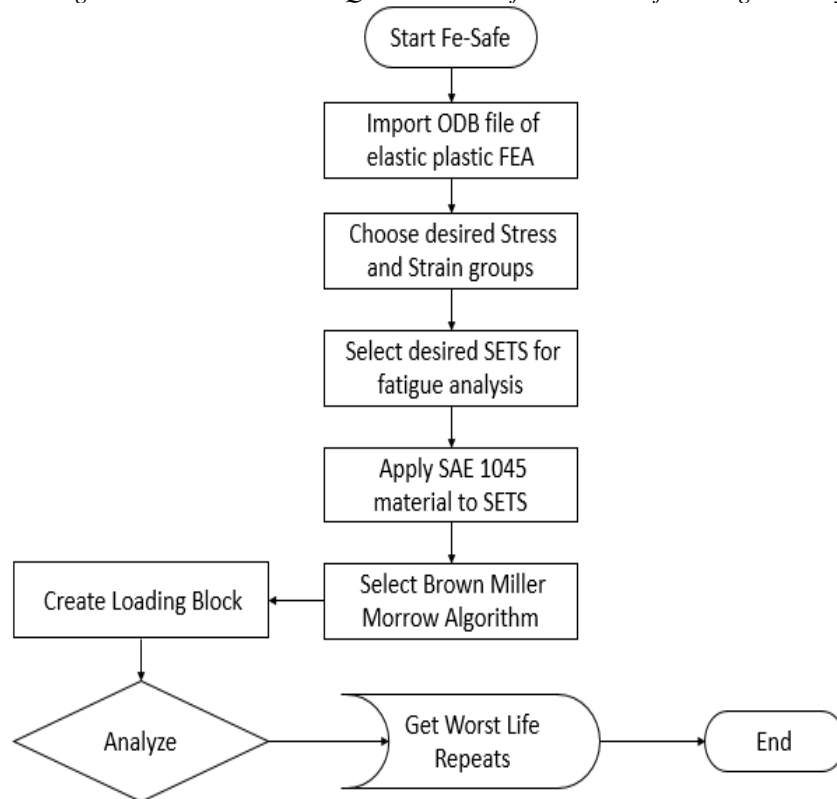*Figure XII. Combined ABAQUS and Fe-Safe Flowchart for Fatigue Analysis*

Figure XIII. Fe-Safe Fatigue Life Prediction Flow Chart

The schematic illustration of fatigue analysis utilizing ABAQUS and Fe-Safe is shown in **Figure XII**. It is known for its accuracy, speed, and ease of use when analyzing metals, rubber, thermo-mechanical and creep fatigue, and welded joints. Fe-Safe is a robust, all-inclusive, and user-friendly packages of fatigue analysis tools for finite element models [37]. The flowchart for Fe-Safe working is shown in **Figure XIII**. The worst life repeats represent the number of cycles to failure for estimation of fatigue life of joint.

3. Results & Discussion. - This chapter includes the results and discussions of outcomes obtained from the above-mentioned methodologies. Results are shown in the form of contours, tables, graphs, or curves. First, the 3D geometry of Load-carrying Cruciform Joint (LCJ) is discussed and then after that, the loading scenarios and boundary conditions for 2D are detailed.

3.1 Results of 3D Geometry. - As mentioned in the previous chapter that this geometry has been studied for five different loadings and only one type of boundary condition. This was done to understand the fatigue analysis process using ABAQUS and Fe-Safe to perform a detailed study on different loading and boundary conditions for 2D geometry. In this context, five loadings are applied on 3D geometry ranging from 480 to 680, and the contour shown in **Figure XIV** is for the last loading value i.e., 680 MPa. **Figure XV** shows the results of fatigue life obtained by Fe-Safe.
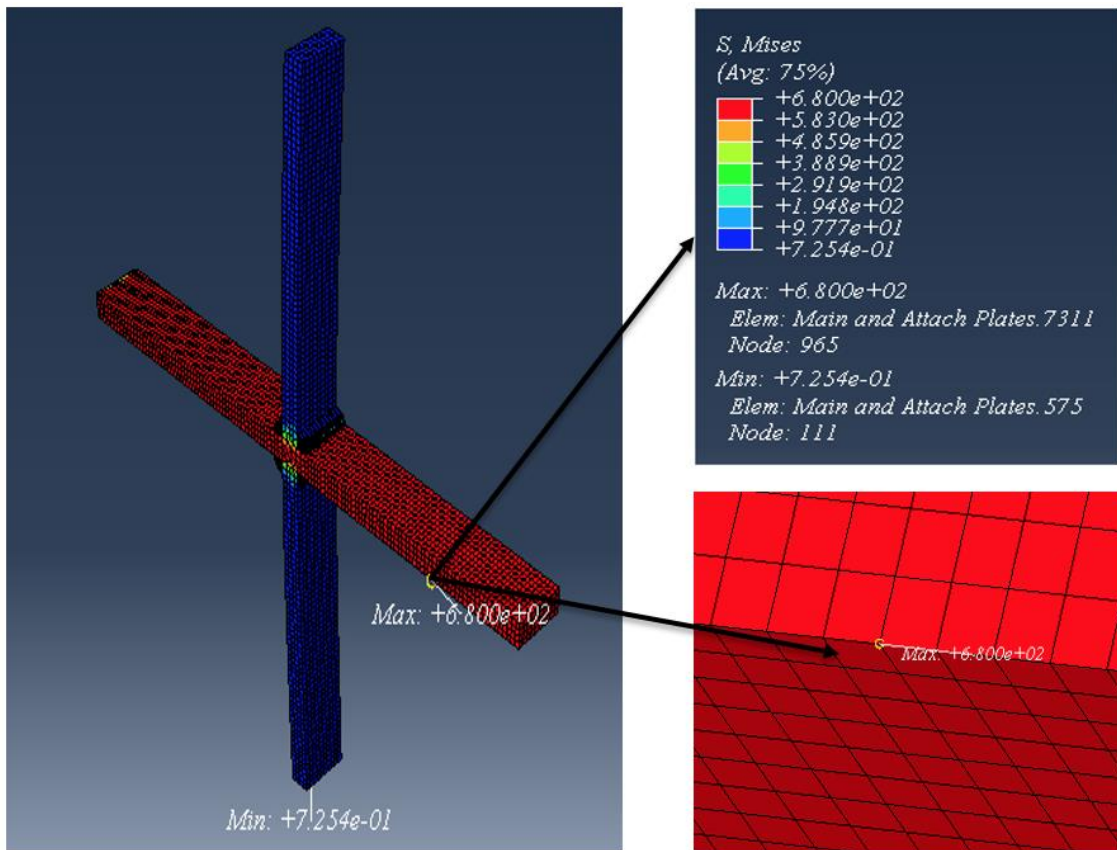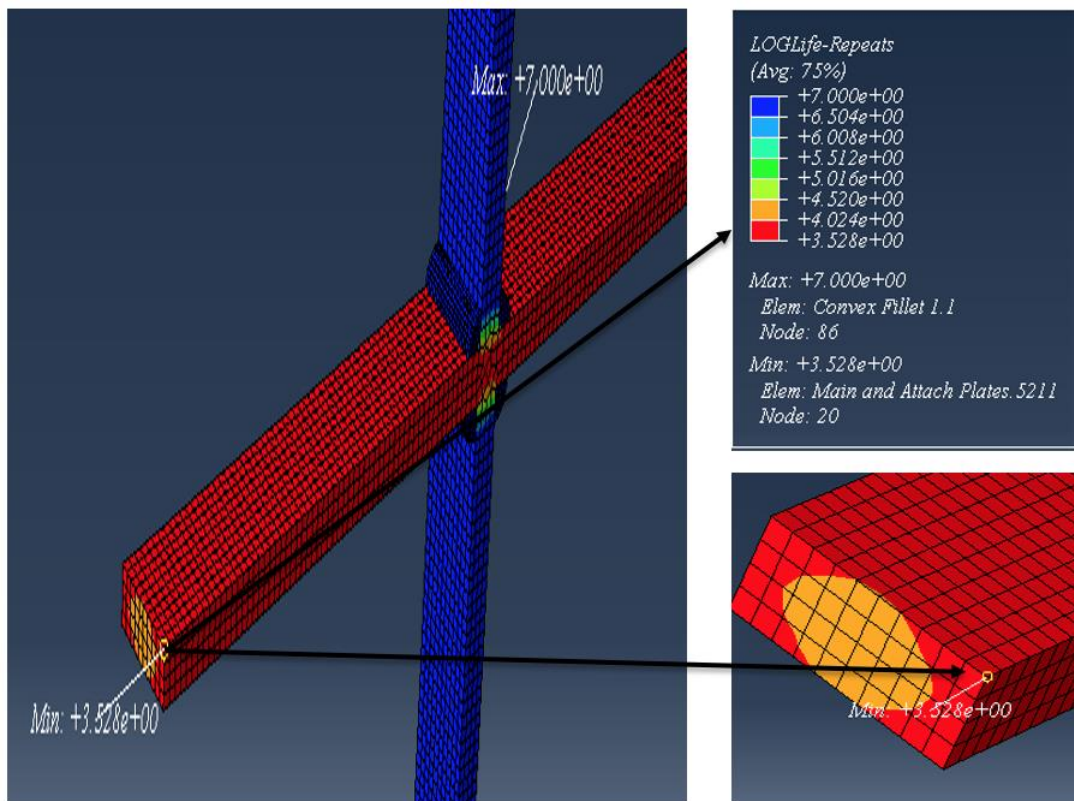
Figure 1: Contour of 3D Geometry for 680 MPa from ABAQUS

Figure 2: Fatigue Life for 3D Geometry obtained from Fe-Safe

3.2 Discussion. - Linear hexahedral elements of type C3D8R are used for the Meshing of 3D geometry. The total number of elements and nodes are 12640 and 17613. The boundary conditions are applied in such a way that the plate end opposite to the applied load is fixed while the other top and bottom ends are allowed to move in the direction of applied stress regarding **Figure 10**. From **Figure 14**, the most crucial region exists on the main plate where the value of Von Mises stress is 680 MPa. It is on element 7311 having node 965. So, one can say that a joint failure will occur on that element. But it is not on the same element as shown by **Figure 15**. According to this, element 5211 with node 20 has minimum Log Life which means that failure occurs on that element, not on element 7311. This element lies in the fixed end region as is clear in **Figure 15**. Log Life repeats are used for representing the number of cycles to failure. The minimum value of Log Life shows that such element or region will fail earlier than other elements or regions of a structure. Hence, as a result, structure damage occurs after a certain number of repetitions of the applied load. **Table 5** contains outcomes for each applied load.
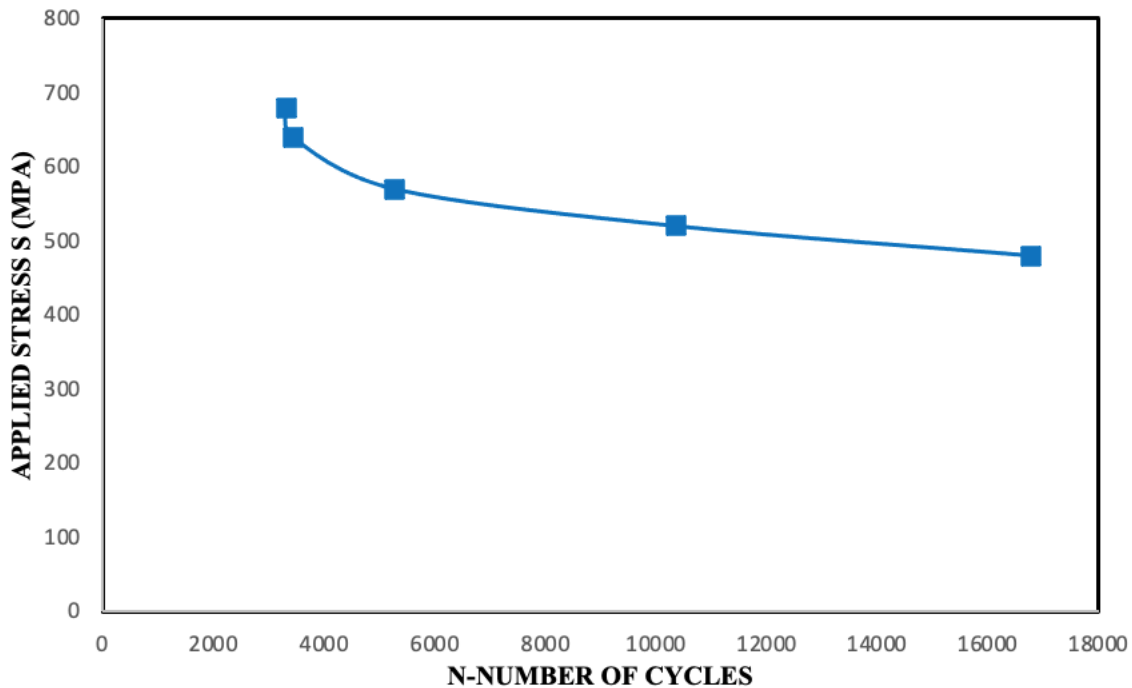

Figure XVI. SN-Curve for 3D Geometry of Joint

Results for 3D Geometry	
Applied Stress (MPa)	No. of Repeats
480	16773.326
520	10354.495
570	5281.393
640	3448.218
680	3318.614

Table V. Number of Repeats for each Applied Load on 3D Geometry

Using values of **Table V**, a graph is made to represent SN-Curve for 3D geometry of Cruciform joint. See **Figure XVI**.

3.3 Results of 2D Geometry. - For 2D geometry, the axial load applied ranges from 100 to 500 MPa with an equal difference of 100 MPa. But, for each case, only the outcomes obtained after applying maximum load i.e. 500 MPa are shown in the following figures. It is chosen because, at maximum value, it is better to study the structural changes occurred in the joint to show extreme behavior at higher loading condition. See **Figure XVII** for results obtained from elastic-plastic FEA in ABAQUS and **Figure XVIII** for the number of cycles got from Fe-Safe.
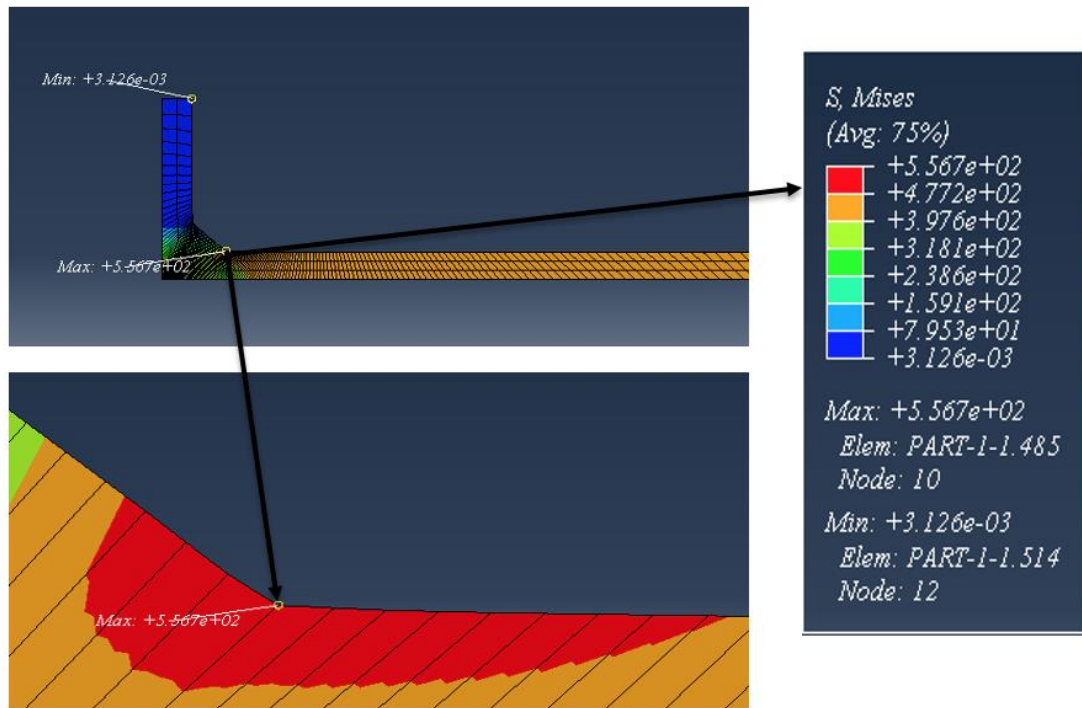
Figure XVII. Contour of Axial Load of 500 MPa from ABAQUS

3.4 Discussion. - Quadratic quadrilateral elements of type CPE8R are used for the Meshing of 2D geometry. The total number of elements and nodes are 547 and 2036. The boundary condition type 1 is such that in which 1/4ᵗʰ of 2D geometry is considered due to symmetry for elastic-plastic FEA and in which attached plate end opposite to applied stress is allowed to move in the vertical direction and the lower end of main plate is allowed to move in the horizontal direction. From **Figure XVII**, the most critical area exists on fillet weld toe where the value of Von Mises stress is 556.2 MPa. It is on element 485 having node 10. So, it is obvious to say that joint damage will occur to that element. And it is the same element as shown in **Figure XVIII**. According to this, element 485 with node 10 has minimum Log Life repeats which means that failure occurs on that element. This element lies in the weld toe region as is clear in **Figure XVIII**. Log Life repeats are used for signifying the number of cycles to failure. **Table VI** contains the results for each applied axial load.
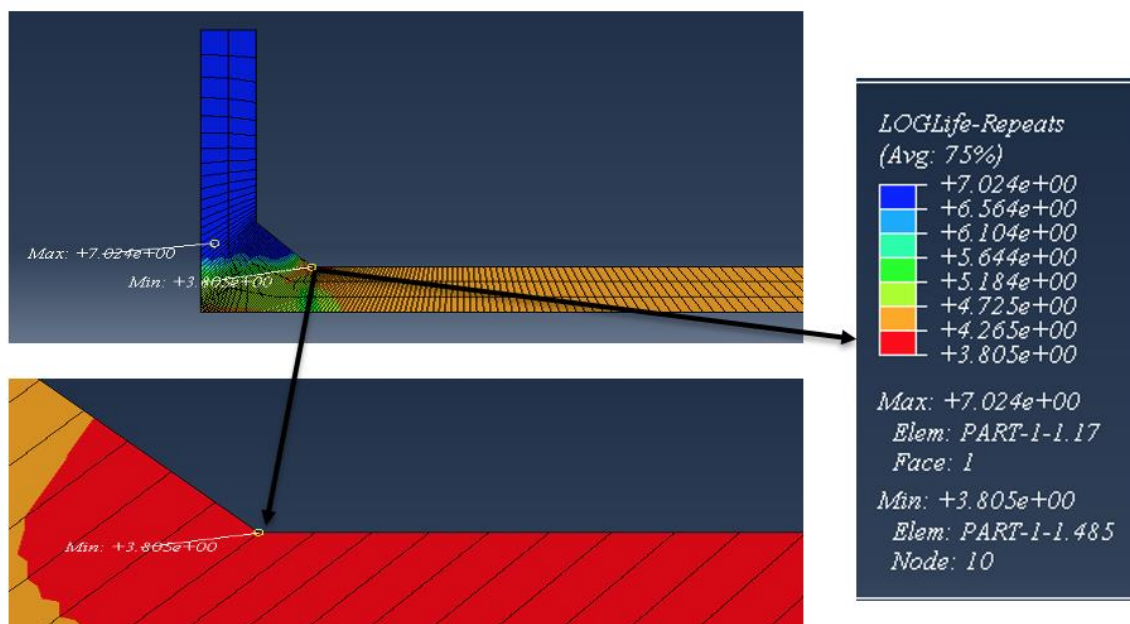
Figure XVIII. Fatigue Life for Axial Load of 500 MPa obtained from Fe-Safe

Results for Axial loading	
Applied Stress (MPa)	**No. of Repeats**
480	432123.5
520	347315.469
570	21706.598
640	6183.626
680	6141.355

Table VI. Number of Repeats for Axial Load on 2D Geometry

Using values of **Table VI**, SN-Curve for axial loading is made. See **Figure XIX**.
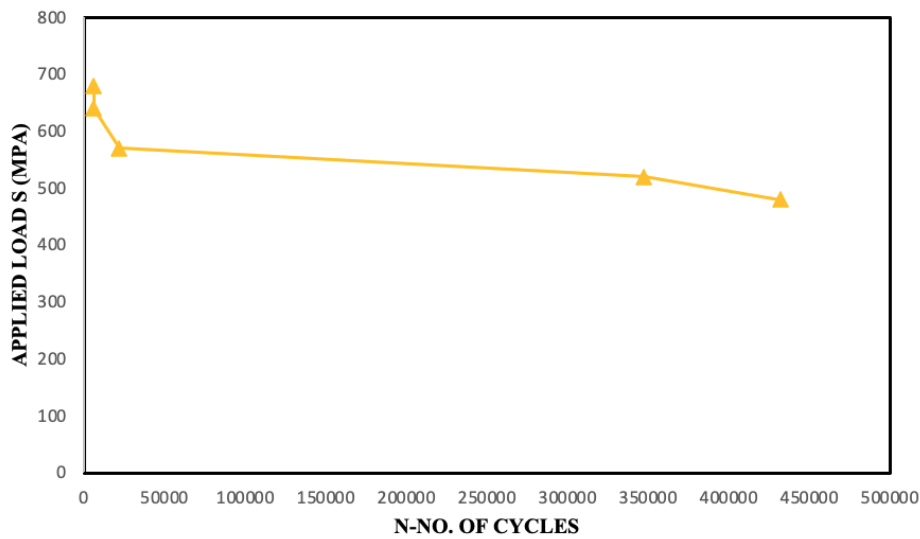
Figure XIX. SN-Curve for Axial loading applied 2D Geometry.

3.5 Comparison of Results (3D & 2D Geometry). - Comparison of results for 3D and 2D geometry is shown in **Figure XX** for better understanding of the trends of SN-curves. At load 480 MPa, there is large difference between number of cycles of both geometry and when becomes closer to 600 MPa, the curves for both begin coinciding with each other. It means both geometries show the same fatigue behavior at higher loadings when consider strain-based Brown Miller Model for fatigue estimation.

Figure 3: Comparison of Results

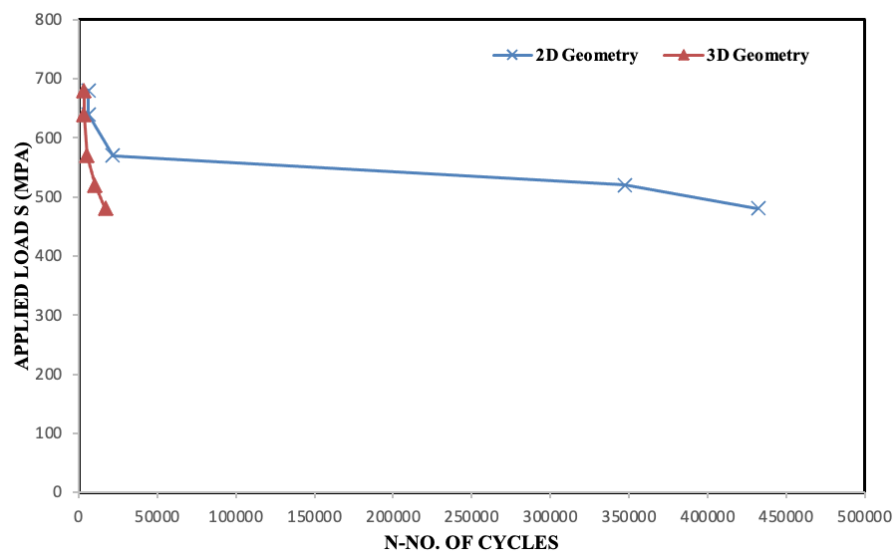**4. Validation Study. -** For validation study of methodology, the data are taken from [38]. The data is composed of eight different geometrical configurations of welded Cruciform joints. Each joint has four welds with different horizontal and vertical dimensions. See **Figure XXI** for a 3D geometry description.

Dimensions of each weld detail for eight samples are given **Table VII**. The sample numbers used in that table are the same as in **Table II** of [11]. The width of the main plate is denoted by "L" and the thickness of the attached plates is indicated by "t". All the dimensions are in millimeters (mm).
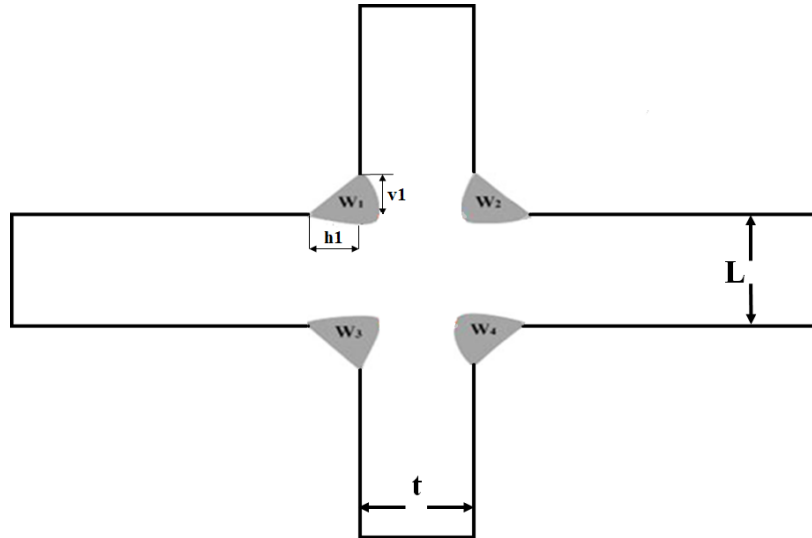

Figure XXI. Description of symbols used for geometry.

Sample No.	Weld 1 (mm)		Weld 2 (mm)		Weld 3 (mm)		Weld 4 (mm)		L	t
	h1	v1	h2	v2	h3	v3	h4	v4	(mm)	(mm)
19	8.13	8.52	7.25	8.6	8.5	8.62	7.8	9.63	35	12
6	10.27	10.36	9.82	11.56	9.9	11.9	8.85	10.21	35	12
5	10.57	10.52	10.11	12.94	10.08	12.08	9.05	9.87	35	12
4	10.19	10.21	10.56	11.89	10.49	11.38	8.82	9.9	35	12
18	8.89	12.33	6.91	10.94	10.49	11.1	10.8	11.93	35	12
3	10.27	10.36	9.82	11.56	9.9	11.9	8.85	10.21	35	12
2	10.57	10.52	10.11	12.94	10.08	12.08	9.05	9.87	35	12
1	10.19	10.21	10.56	11.89	10.49	11.38	8.82	9.9	35	12

Table VII. Details of Eight Samples used for the validation study

4.1 Experimental Data. - Experimental data contain the number of fatigue cycles, location of the fracture, and applied loads concerning each sample mentioned in **Table VII**. Experimental data are given in **Table VIII**.

Sample Number	Cases	Applied Load (MPa)	Fatigue Cycles	Fracture Location
19	C1	100	320500	Weld Root
6	C2	200	224700	Weld Toe
5	C3	240	129600	Weld Toe
4	C4	280	56580	Weld Toe

18	C5	305	53500	Weld Toe
3	C6	320	46800	Weld Toe
2	C7	360	37800	Weld Toe
1	C8	400	21500	Weld Toe

Table VIII. Experimental data detail

A 250-KN electro-hydraulic servo testing machine MTS 809 coupled with a load-control condition was used to conduct higher cycle fatigue experimentations of load-carrying Cruciform joint.

4.2 Material for Joint. - The SAE 1045 is the material used in this study. It is mild carbon steel that is widely utilized in a variety of industries. Axles, bolts, connecting rods, pins, studs, shafts, spindles, and other similar uses are common. It is obvious that these parts are frequently subjected to repeated loading. As a result, increasing the fatigue resistance of SAE 1045 appears to be necessary. SAE 1045's chemical composition is obtained from [33] and is presented in **Table IX**.

Constituents	Carbon	Silicon	Manganese	Phosphorus	Sulfur	Iron
Weight %	0.423	0.20	0.56	0.008	0.02	rest

Table IX. SAE 1045 Chemical Composition

The monotonic characteristics are achieved [34] by utilizing a 25 KN servo-hydraulic machinery to perform a uniaxial cycle test with a stress ratio of R = -1. During the test, a 2-mm strain gauge was affixed to the specimen to gather strain events. See **Table X** for SAE 1045 monotonic properties.

Properties	Values
Ultimate Tensile Stress (σ_u)	798 MPa
Yield Stress (σ_y)	414 MPa
Young's Modulus (E)	198 MPa

Table X. SAE 1045 Monotonic Properties

Following that, a cycle test [34] was performed at various percentages of UTS (ultimate tensile strength) acquired from the preceding tensile test. The percentages used are 60, 65, 70, 80, and 85 percent. As a result, five various stress values were used to capture failure time and strain range readings. See **Table XI** for more information.

Applied Stress (MPa)	Strain Ranges ($\mu\varepsilon$)
480 (60 % of UTS)	2294
520 (65 % of UTS)	3200
570 (70 % of UTS)	4059
640 (80 % of UTS)	4565
680 (85 % of UTS)	5800

Table XI. Applied Stresses for Cyclic Test and Strain Ranges

4.3 Conducting Elastic-Plastic FEA. - ABAQUS is used for elastic-plastic finite element analysis. First, the 3D geometry of a cruciform joint is created in ABAQUS using the Sketch and Feature tools. Static General STEP is built for plastic analysis after specifying the elastic and plastic material characteristics of SAE 1045. In the current case, eight distinct types of geometrical configurations are investigated for fatigue cycles, for loading values of 100, 200, 240, 280, 305, 320, 360, and 400 for the same boundary condition. For Meshing, an 8-node linear hexahedral element of type C3D8R with reduced integration is utilized. The whole flow diagram of boundary and loading conditions can be seen in **Figure XXII**. The right and left ends are allowed to move in x, y and z direction while all rotations are forbidden. On the upper and lower end of the joint load is applied. The loading nature is cyclic tensile, and zero weld penetration is considered because of the technique of wire electrode cutting [11]. All eight configurations were made separately keeping the other dimensions constant.
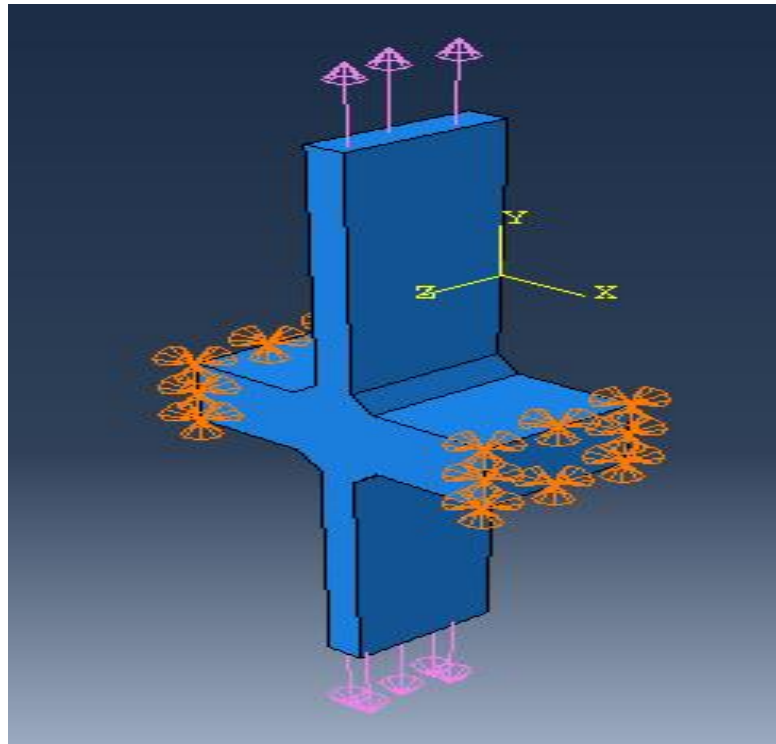
Figure XXII. Loading and boundary conditions on cruciform joint.

4.4 Fatigue Analysis Using Fe-Safe. - Fe-safe is the industry's first commercially accessible fatigue analysis program that focuses on current multiaxial strain-based fatigue methodologies. The schematic illustration of fatigue analysis utilizing ABAQUS and Fe-Safe is shown in **Figure XXIII**. It is known for its accuracy, speed, and ease of use when analyzing metals, rubber, thermo-mechanical and creep fatigue, and welded joints. Fe-Safe is a robust, all-inclusive, and user-friendly packages of fatigue analysis tools for finite element models [37]. The worst life repeats represent the number of cycles to failure for estimation of fatigue life of joint.
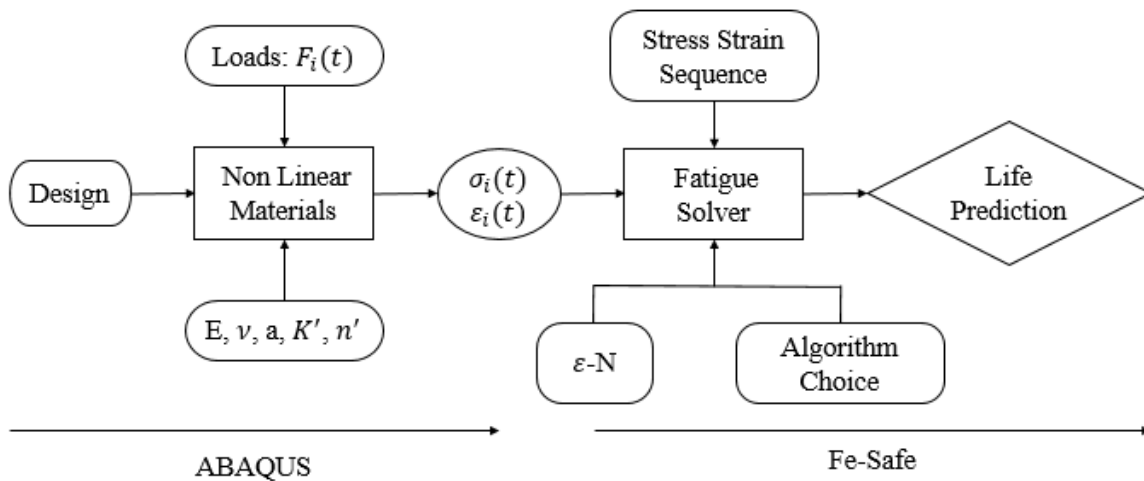

Figure XXIII. Fatigue analysis using ABAQUS and Fe-Safe

4.5 Simulation Results. - The simulated results are shown in the form of Log Life repeats contours. **Figure XXIV** contains contours of each eight configurations for their respective loadings i.e., 100, 200, 240, 280, 305, 320, 360, 400 MPa. Each contour indicated the region in which minimum Log Life repeats occur with a highlighted area. For all cases, the fatigue damage location is not the same because of the irregular or nonlinear plastic nature of the material. After that, **Table XII** is made to show the differences between the simulated and experimental number of cycles, percentage errors, and the failure locations for eight samples. Finally, **Figure XXV** shows a graph representing both simulated and experimental curves.
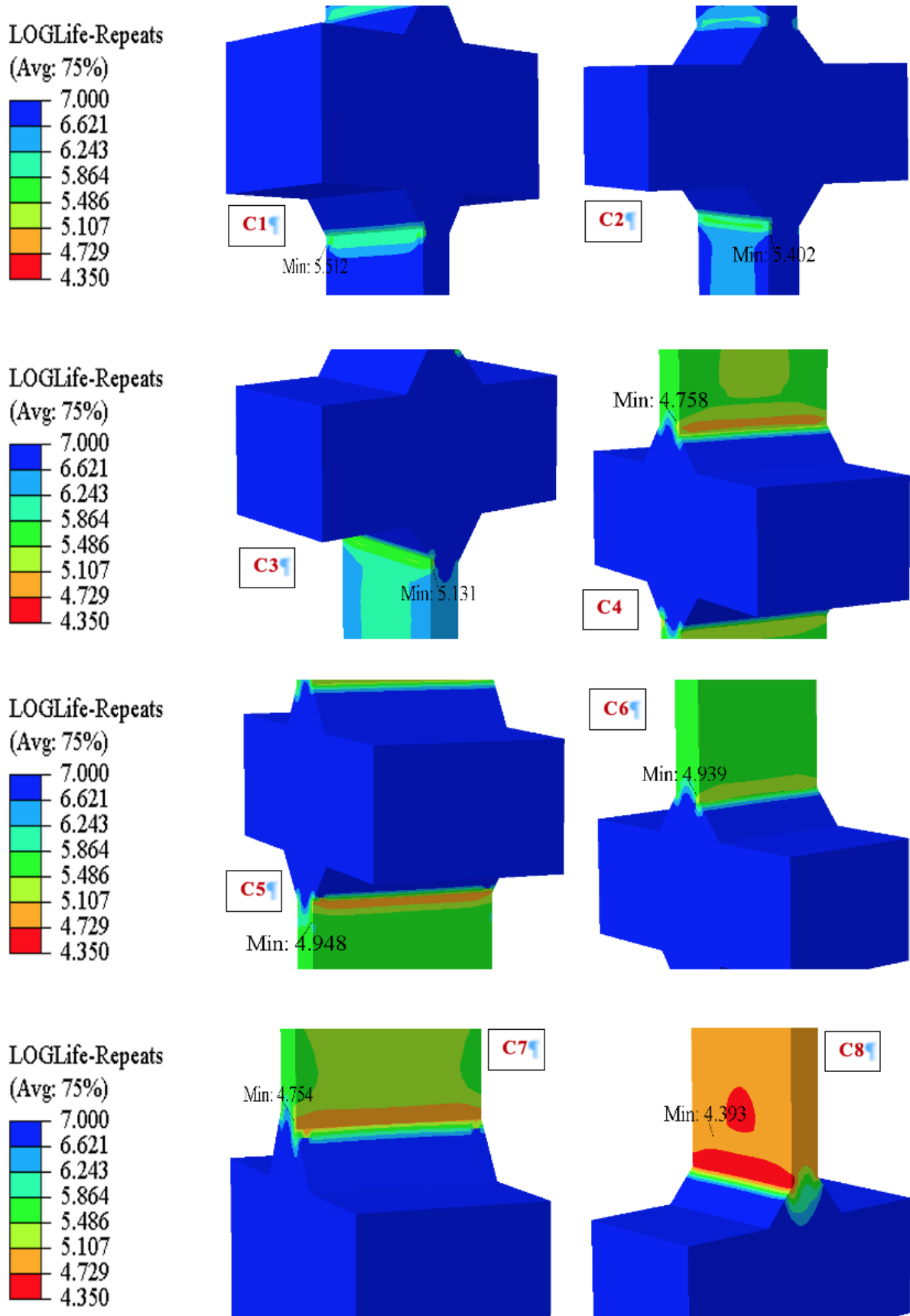
Figure XXIV. Simulated results for all samples by ABAQUS and Fe-Safe

Sample Number	Applied Load (MPa)	Simulated Cycles	Experimental Cycles	% Error	Fracture Location
19	100	324776	320500	1.316	Weld 3 Toe on the lower plate
6	200	234804	224700	4.303	A little bit below of Weld 4 Toe on the lower plate
5	240	135127	129600	4.090	Weld 4 Toe on the lower plate
4	280	57215	56580	1.109	On upper Plate above Weld 2
18	305	56794	53500	5.799	Lower Plate below weld 3
3	320	50186	46800	6.746	The backside of the upper plate above weld 1
2	360	38610	37800	2.097	The backside of the upper plate above weld 1
1	400	21648	21500	0.683	Near to back end on the upper plate

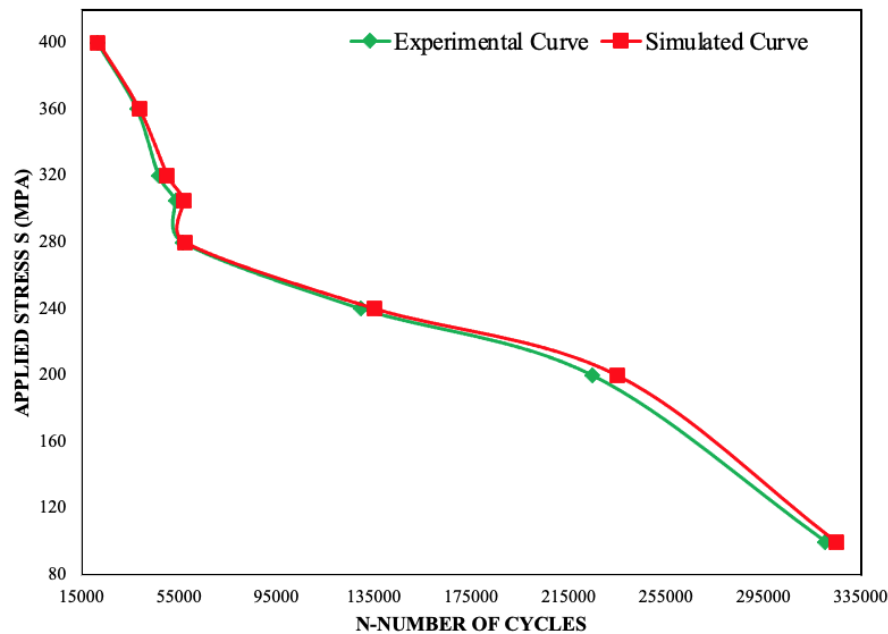*Table XII. Detail of Simulations for Eight samples.*

Figure XXV. Simulated and Experimental SN-Curve

5. Conclusions. - The conclusions for 3D geometry, 2D geometry and validation study are as follows:

5.1 3D Geometry. –

- The fatigue failure occurs on that element that did not lie on the lower surface of the main plate. Rather, it lied on the fixed end of the main plate.
- Although the whole plate is under extreme loading as shown in **Figure XIV**, the accumulated effect of applied load cause failure only on the element of the fixed end side.
- As stated, earlier results of only the higher loadings were displayed, so, it may be possible that in other cases the element of failure would not be the same.

- The SN-Curve for 3D geometry shows large differences in the number of repeats for small loading values i.e., from 480 to 640 MPa.

- When the load of 680 MPa was applied, the fatigue damage occurred rapidly after a few repeats showing a very small difference as compared to previous values.

- The abrupt fatigue failure due to large load is also making the sense of corresponding to larger load applications.

5.2 2D Geometry. –

- The applied load causes tension in the weld joint; opposite to the case of 3D geometry, in which applied load cause compression.

- The most affected zone due to tension is at the weld toe. The same region is also highlighted by Fe-Safe results.

- The SN-Curve for this case showed huge differences between the number of repeats when the applied loads were small.

- The difference became small as the load exceeded 500 MPa indicating the occurrence of fatigue damage after a few thousand repeats as compared to small loads.

- This is true because higher loads cause faster plastic deformation accompanied by large strains.

5.3 Validation Study. - Following are the key findings with reference to **Table XII** and **Figure XXV**:

- The simulated results show that the fracture locations are different for most of the samples from the region obtained by experimental results.

- The number of cycles attained after the simulation is greater than the experimental for each sample.

- Most of the fracture locations are identified near the weld toes region except for toes of weld 3 and weld 4.

- No weld root failure has been identified for any weld and no failure occurs for toes of weld 1 and weld 2.

- The lower plate is in a severe situation because weld 3 and weld 4 are located on lower plate, joining the main plate.

- Since no fracture occurred on weld 1 and weld 2, the most crucial region for upper plate is the backside of the plate.

- No fracture occurred on the main plate and toes of welds situated on the main plate because loading is tensile causing fracture on weld toes situated on upper & lower plates and on the lower & upper plates separately.

- The graph in **Figure 25** shows that at higher loads, fatigue failure occurs after few thousand repeats due to abrupt plasticity behavior in material and for lower loads, it takes more than 3 lacs repeats.

- The lowest % error is 0.683 for Sample 1 with 400 MPa load and maximum % error is 6.746 for Sample 3 with 320 MPa load after simulation.

- As the % error is less than 10 % for all cases, it shows that the simulated results by ABAQUS and Fe-Safe are in acceptable range.

6. Recommendations. - Recommendations for improving designs of load carrying cruciform joints (LCJs) and for future research directions are as follows:

6.1 Improving Design of Load Carrying Cruciform Joints. -

- Increasing the radius of the weld toe helps minimize stress concentration, which is a typical site for fracture development.

- Adjusting weld leg length helps equally distribute loads throughout the joint and reduce localized stress concentrations.

- Weld reinforcement, like thicker welds or fillet connections, can improve joint strength.

- High-quality welding techniques, including joint preparation, weld parameters that are and post-weld examination, can reduce weld faults that cause stress.

- Applying post-weld procedures, such as peening or thermal treatment, can lower residual stresses in the connecting surfaces and prevent early fatigue cracks.

6.2 Future Research Directions. -

- Consider using modern materials like high-strength steels, aluminum alloys, as well as fiber-reinforced composites to manufacture • cruciform joints.

- Investigate how material parameters, which include the tensile strength, yield strength, and resistance to fatigue, affect joint load-carrying capability and fatigue life.

- Incorporate more complicated loading situations, such as coupled axial, bending, as well as torsional loads, that ship constructions often face.

- Use sophisticated fatigue analysis approaches, such as critical plane techniques or energy-based theories, to properly simulate joint performance for multi-axial fatigue loading.

- Investigate how environmental factors such corrosive sea environments, temperature changes, and weathering impact the functionality and endurance of cruciform joints.

- Understand how additive manufacturing (AM) methods, such 3D printing, may be used to create cruciform joints with customizable attributes and increased geometric complexity.

- Investigate how AM-specific factors, including roughness of the surface and residual stresses, affect joint's mechanical efficiency and fatigue life.

References

[1] D. W. a. J. L. Chuntong Li, "Numerical analysis and experimental study on the scaled model of a container ship lashing bridge," Ocean Engineering, vol. 201, no. March, p. 107095, 2020.

[2] K. Y. L. P. a. Y. G. Jingxia Yue, "A frequency-time domain method for ship fatigue damage assessment," Ocean Engineering, vol. 220, no. August 2020, p. 108154, 2021.

[3] W. Fricke, "Fatigue and Fracture of Ship Structures," Encyclopedia of Maritime and Offshore Engineering, pp. 1-12, 2017.

[4] A. P. MSP. Raju, "A Study on Common Ship Structural Failures," International Journal of Mechanical Engineering and Technology, vol. 9, no. 7, pp. 746-754, 2018.

[5] K. H. Yang, "Chapter 2 - Meshing, Element Types, and Element Shape Functions," in Basic Finite Element Method as Applied to Injury Biomechanics, K. Yang, Ed., Academic Press, 2018, pp. 51-109.

[6] S. V. B. P. Shwetha K, "Comparison Between Thin Plate And Thick Plate From Navier Solution Using Matlab Software," International Research Journal of Engineering and Technology, vol. 05, no. 06, pp. 2675-2680, June 2018.

[7] A. Risitano, "Welded Joints," in Mechanical Design, CRC Press, 2011, pp. 463-486.

[8] J. K. Janusz Kozak, "The Influence of Manufacturing Oversizing on Postwelding Distortions of the Fillet Welded Joint," Polish Maritime Research, vol. 22, no. 4, pp. 59-63, 2015.

[9] S. Chakraborty, "Common Welding Methods And Weld Defects In Shipbuilding Industry," Marine Insight, 9 July 2021. [Online]. Available: https://www.marineinsight.com/naval-architecture/common-welding-methods-weld-defects-shipbuilding-industry/.

[10] B.-S. J. a. S.-W. K. Tae-Jun Kim, "Welding Deformation Analysis Based on Improved Equivalent Strain Method to Cover External Constraint During Cooling Stage," International Journal of Naval Architecture and Ocean Engineering, vol. 7, no. 5, pp. 805-816, 2015.

[11] X. L. a. S. R. Wei Song, "Fatigue assessment of steel load-carrying cruciform welded joints by means of local approaches," Fatigue & Fracture of Engineering Materials and Structures, vol. 41, no. 12, pp. 2598-2613, 2018.

[12] Wikipedia, "Welding Joint," 1 January 2021. [Online]. Available: https://en.wikipedia.org/wiki/Welding_joint#cite_note-7.

[13] N. T. T. Y. A. T. a. A. Y. Iwata Toshiaki, "Thickness effect on fatigue strength of welded joint improved by HFMI," Yosetsu Gakkai Ronbunshu/Quarterly Journal of the Japan Welding Society, vol. 34, no. 4, pp. 249-259, 2016.

[14] J. S. Zuheir Barsoum, "Fatigue assessment of cruciform joints welded with different methods," Steel Research International, vol. 77, no. 12, pp. 882-888, 2006.

[15] T. a. C. K.Saiprasertkit, "Experimental study of load-carrying cruciform joints containing incomplete penetration and strength under-matching in low and high cycle fatigue regions," Procedia Engineering, vol. 14, pp. 572-581, 2011.

[16] T. O. a. Y. K. Kazuki Tatsuta, "A study on the size effect of cruciform joint for fatigue strength subjected to bending and axial stress," in Japan Society of Naval Architects Lecture Proceedings No. 22, 2016.

[17] P. G. J. J. J. R. a. P. L. Heikki Remesa, "Fatigue strength modelling of high-performing welded joints," International Journal of Fatigue, vol. 135, no. February, p. 105555, 2020.

[18] X. F. P. a. H. W.Song, "Fatigue failure transition analysis in load-carrying cruciform welded joints based on strain energy density approach," Fatigue and Fracture of Engineering Materials and Structures, vol. 40, no. 7, pp. 1164-1177, 2017.

[19] W. a. C. C.Fischer, "Fatigue assessment of web-stiffened corners in plated structures by local approaches," Ship Technology Research, vol. 65, no. 2, pp. 69-78, 2018.

[20] X. L. Wei Song, "High cycle fatigue assessment of steel load-carrying cruciform welded joints: An overview of

recent results," Frattura ed Integrita Strutturale, vol. 12, no. 46, pp. 94-101, 2018.

[21] N. A. Oscar Araque, "Weld magnification factor approach in cruciform joints considering postwelding cooling medium and weld size," Materials, vol. 11, no. 81, pp. 1-18, 2018.

[22] N. O. Toru Shiratsuchia, "Investigation of thickness and bead profile effects on fatigue strength of welded joints based on relative stress gradient," International Journal of Fatigue, vol. 134, no. February, p. 105520, 2020.

[23] Y. L. a. S. T. Yixun Wang, "Parametric formula for stress concentration factor of fillet weld joints with spline bead profile," Materials, vol. 13, no. 9, p. 4639, 2020.

[24] P. T. a. G. G. Krzysztof L.Molski, "Stress concentration at cruciform welded joints under axial and bending loading modes," Welding in the World, vol. 64, no. 11, pp. 1867-1876, 2020.

[25] K.-H. C. a. S. M. Wang Sub Shin, "Fatigue analysis of cruciform welded joint with weld penetration defects," Engineering Failure Analysis, vol. 120, no. November 2020, 2021.

[26] D. S. G. R. F. B. Pietro Foti, "Fatigue assessment of cruciform joints Comparison between Strain Energy Density predictions and current standards and recommendations," Engineering Structures, vol. 230, no. November 2020, 2021.

[27] Z. D. J. C. X. J. J. D. Yang Peng, "Fatigue behaviour of load-carrying fillet-welded cruciform joints of austenitic stainless steel," Journal of Constructional Steel Research, vol. 2021, 2021.

[28] P. W. a. H. F. Jianxiao Ma, "Fatigue life of 7005 aluminum alloy cruciform joint considering welding residual stress," Materials, vol. 14, no. 5, pp. 1-20, 2021.

[29] X. L. a. S. T. L. Haisheng Zhao, "Fracture analysis of load-carrying cruciform welded joint with a surface crack at weld toe," Engineering Fracture Mechanics, vol. 241, no. July 2020, pp. 1-21, 2021.

[30] X. L. G. Z. S. W. D. S. M. H. a. F. B. Wei Song, "Notch energy-based low and high cycle fatigue assessment of load-carrying cruciform welded joints considering the strength mismatch," International Journal of Fatigue, vol. 151, p. 106410, 2021.

[31] M. D. A. A. a. T. B. Hamidreza Rohani Raftar, "Re-evaluation of weld root fatigue strength for load-carrying fillet welded joints using the notch stress concept," International Journal of Fatigue, vol. 144, no. November 2020, 2021.

[32] W. W. R. F. P. Z. a. Y. D. Zhiyu Jie, "Stress intensity factor and fatigue analysis of cracked cruciform welded joints strengthened by CFRP sheets considering the welding residual stress," Thin Walled Structures, vol. 154, 2020.

[33] N. Y. A. E. Sasan Yazdani, "Enhancement of fatigue strength of SAE 1045 steel by tempering treatment and shot peening," Materials Science Forum, Vols. 561-565, no. PART 1, pp. 41-44, 2007.

[34] S. A. N. J. O. I. Mazian Mohammad, "Fatigue life assessment of SAE 1045 carbon steel under strain events using the Weibull distribution," Journal of Mechanical Engineering, vol. 5, no. Specialissue 1, pp. 165-180, 2018.

[35] D. S. SIMULIA, "Chapter 7 - Biaxial Fatigue," in Fatigue Theory Reference Manual, Dasault Systems, 2021, pp. 1-57.

[36] D. S. SIMULIA, "Chapter 14 - Fatigue Analysis of Elastic FEA Results," in Fe-Safe 2019 User Guide, Dasault Systems, 2018, pp. 1-26.

[37] D. S. SIMULIA, "Chapter 1 - Introduction," in Fe-Safe 2019 User Guide, Dasault Systems, 2018, pp. 1-6.

[38] X. L. S. Wei Song, "Fatigue assessment of steel load-carrying cruciform welded joints by means of local approaches," Fatigue and Fracture of Engineering Materials and Structures, vol. 41, no. 12, pp. 2598-2613, 2018.

Nota contribución de los autores:

1. Concepción y diseño del estudio
2. Adquisición de datos
3. Análisis de datos
4. Discusión de los resultados
5. Redacción del manuscrito
6. Aprobación de la versión final del manuscrito

ZMM ha contribuido en: 1, 2, 3, 4, 5 y 6.
MA ha contribuido en: 1, 2, 3, 4, 5 y 6.
SAAZ ha contribuido en: 1, 2, 3, 4, 5 y 6.

Nota de aceptación: Este artículo fue aprobado por los editores de la revista Dr. Rafael Sotelo y Mag. Ing. Fernando A. Hernández Gobertti.